DOI 10.1007/s10778-020-00995-y
International Applied Mechanics, Vol. 56, No. 1, January, 2020

STABILITY OF A SANDWICH CYLINDRICAL SHELL WITH CORE SUBJECT TO EXTERNAL PRESSURE AND PRESSURE IN THE INNER CYLINDER*

N. P. Semenyuk and N. B. Zhukova

A generalized design model is proposed to study the stability and initial post-buckling equilibrium trajectory of sandwich cylindrical shells with elastic core that resists only transverse tension–compression. The model includes nonlinear equilibrium mixed-form equations, asymptotic equations obtained by the Koiter–Budiansky method, and the analytical solution of a homogeneous eigenvalue problem and inhomogeneous problem to find the values of the unknown functions at the critical point. The numerical results obtained indicate that the internal pressure strongly influences the critical load and initial post-buckling behavior of the shells.

Keywords: stability, post-buckling behavior, sandwich shells, external pressure, pressure in inner cylinder, Koiter–Budiansky asymptotic method

Introduction. Sandwich shells with core have inhomogeneous structure whose typical feature is that the core greatly differs from the face layers not only in thickness but also in mechanical properties. As a rule, the core layer has much greater thickness and much lower elastic modulus and specific density. Methods for analysis of the strength and stability of sandwich shells are outlined in [1, 4, 9, 11, 12, 15]. Many practical solutions indicate that sandwich shells are mainly used in aircraft [15, 19].

The history of sandwich shells, their advantages over monocoque shells, current use, and prospects for future use are detailed in [15].

There is a need to study sandwich shells with core that is elastic only in the transversal direction. If the face layers interact through linear springs perpendicular to their surface, then the equivalent continuous body will have such properties. In [16], a model with springs between layers of a two-wall nanotube is used to describe the interaction caused by the Van der Waals attraction-repulsion forces. Sandwich-shell systems can also be considered as optimal for such structures as underwater submersibles and pipelines. It is necessary to change the design model [4] because the inner layer is subject to not only the surface pressure exerted by the outer layer through the core, but also the pressure of opposite sign exerted by the substance in the inner cylinder [18] or the fluid or gas in underwater pipelines.

In what follows, we will develop some aspects of the theory of sandwich shells of this type. We will use the modified variational Lagrange principle to derive the governing equations for sandwich shells, and will use a continuous model of a body that is elastic only in the traverse direction to describe the core [1, 3, 4]. The equations will be derived without any additional hypotheses except for those typical for shell theory. The continuous equations of multi-wall nanotubes [7, 13, 14, 16, 17] have the same structure as those of the theory of multilayer shells derived without a single hypothesis for the whole shell [1–3]. This

S. P. Timoshenko Institute of Mechanics, National Academy of Sciences of Ukraine, 3 Nesterova Str., Kyiv, Ukraine 03057; e-mail: compos@inmech.kiev.ua. Translated from Prikladnaya Mekhanika, Vol. 56, No. 1, pp. 52–66, January–February 2020. Original article submitted October 11, 2018.

* This study was sponsored by the budgetary program Support of Priority Areas of Research (KPKVK 6541230).

also applies to sandwich shells with transverse compliance of the core. These sandwich shells differ by the methods of determining the mechanical characteristics of the core [7, 15].

Using the asymptotic Koiter–Budiansky method [5, 6, 8], we will formulate an eigenvalue problem and an inhomogeneous problem to find the increments of the functions in the initial post-buckling state. We will also derive a formula for a coefficient b used to determine the possible direction of the equilibrium trajectory in the initial post-buckling state and the sensitivity of sandwich shells to the initial geometric imperfections.

The stability and initial post-buckling behavior of composite cylindrical shells were examined in [10].

1. Nonlinear Equilibrium Equations of Sandwich Shells. To derive the nonlinear equilibrium equations of sandwich shells, we will employ the variational Lagrange principle

$$\delta V - \delta A = 0, \tag{1}$$

where V is the strain energy of the shell, A is the work done by the external load. The energy V consists of the energies of the two face layers, V_1 and V_2, and the energy of the core layer, V_3. In accordance with Timoshenko's hypotheses for the strain energy V_i (i = 1, 2), we have

$$V_i = \frac{1}{2}\int_0^L \int_0^{2\pi} \Big(T_{11,i}\varepsilon_{11,i} + T_{12,i}\varepsilon_{12,i} + T_{22,i}\varepsilon_{22,i} + T_{13,i}\varepsilon_{13,i} + T_{23,i}\varepsilon_{23,i}$$

$$+ M_{11,i}k_{11,i} + M_{12,i}k_{12,i} + M_{22,i}k_{22,i} \Big) R_i\, dx d\varphi, \tag{2}$$

where L is the shell length; R_i is the radius of the mid-surface of the ith layer; $T_{mn,i}$ and $M_{mn,i}$ are the forces and moments equivalent to the stresses acting in the layers; $\varepsilon_{mn,i}$ are strains; m and n are indices; $k_{mn,i}$ are the increments of curvatures and torsion.

The force and strain functions are related by Hooke's law as follows:

$$T_{11} = C_{11}\varepsilon_{11} + C_{12}\varepsilon_{12}, \quad T_{12} = C_{66}\varepsilon_{12}, \quad T_{22} = C_{12}\varepsilon_{11} + C_{22}\varepsilon_{22}, \quad T_{13} = C_{55}\varepsilon_{13},$$

$$T_{23} = C_{44}\varepsilon_{23}, \quad M_{11} = D_{11}\varepsilon_{11} + D_{12}\varepsilon_{12}, \quad M_{12} = D_{66}k_{12}, \quad M_{22} = D_{12}k_{11} + D_{22}k_{22}, \tag{3}$$

where C_{mn} and D_{mn} are the shell stiffnesses in tension and bending, respectively [2].

The nonlinear expressions of strains in terms of displacements are adopted in the form following from the Mushtari–Donnell–Vlasov (MDV) theory

$$\varepsilon_{11} = \frac{\partial u}{\partial x} + \frac{1}{2}\theta_1^2, \quad \varepsilon_{12} = \frac{\partial u}{\partial y} + \frac{\partial v}{\partial x} + \theta_1\theta_2, \quad \varepsilon_{22} = \frac{\partial v}{\partial y} - \frac{w}{R_i} + \frac{1}{2}\theta_2^2,$$

$$\varepsilon_{13} = \theta + \theta_1, \quad \varepsilon_{23} = \psi + \theta_2, \quad \varepsilon_{33} = \frac{\partial w}{\partial z}, \quad \theta_1 = \frac{\partial w}{\partial x}, \quad \theta_2 = \frac{\partial w}{\partial y},$$

$$k_{11} = \frac{\partial \theta}{\partial x}, \quad k_{12} = \frac{\partial \theta}{\partial y} + \frac{\partial \psi}{\partial x}, \quad k_{22} = \frac{\partial \psi}{\partial x}, \tag{4}$$

where u and v are the tangential displacements; w is the normal displacement which is positive when directed toward the center of the circle; θ and ψ are the angles of rotation; $y = R_i\varphi$ for the ith layer.

It is assumed that the core (third layer) is perfectly compliant in all the directions, except for the transverse one (along the z-axis). The origin of this axis lies on the mid-surface of the layer. In this case, the strain energy of the third layer is defined as

$$V_3 = \frac{1}{2}\int_0^L \int_0^{2\pi} \int_{-t_3/2}^{t_3/2} \sigma_{33}\varepsilon_{33} R_3\, dx d\varphi dz. \tag{5}$$

The elasticity theory yields:

$$\varepsilon_{33} = \frac{\partial w}{\partial z}, \qquad \sigma_{33} = E_3 \varepsilon_{33}, \qquad \frac{\partial \sigma_{33}}{\partial z} = 0, \tag{6}$$

whence

$$\frac{\partial^2 w}{\partial z^2} = 0, \qquad w = w_0 + z\chi,$$

where χ is a function describing the variation of the displacement w with thickness.

The interfaces conditions at $z = -t_3 / 2$ and $z = t_3 / 2$ are

$$w_1 = w_0 - \frac{t_3}{2}\chi, \qquad w_2 = w_0 + \frac{t_3}{2}\chi,$$

whence

$$w_0 = \frac{w_1 + w_2}{2}, \qquad \chi = \frac{w_2 - w_1}{t_3}. \tag{7}$$

Therefore,

$$\varepsilon_{33} = \frac{w_2 - w_1}{t_3}, \qquad T_{33} = t_3 \sigma_{33} = E_3 t_3 \varepsilon_{33} = E_3 (w_2 - w_1),$$

$$V_3 = \frac{1}{2}\int_0^L \int_0^{2\pi} \frac{E_3}{t_3} (w_2 - w_1)^2 R_3 \, dx d\varphi. \tag{8}$$

The ratio E_3 / t_3 is known to be equal to the modulus of subgrade reaction of a two-dimensional foundation of thickness t_3, disregarding the transverse stresses. Let

$$C_3 = E_3 / t_3.$$

Using Eqs. (2)–(8) of the variational principle (1), where the displacements u_i, v_i, w_i and angles θ_i, ψ_i are assumed to be independent functions, we obtain 10 partial differential equations for the displacements. Application of the tangential strains expressed in terms of displacements (4) in the above variant of the shell theory makes it possible to reduce the governing system of differential equations to eight equations. This system has a mixed form because it contains derivatives of not only displacements but also the force function. Assume that the tangential forces T_{11}, T_{12}, T_{22} appearing in functional (2) are independent in addition to the displacements u, v, w. For the strains ε_{ij} $(i, j = 1, 2)$ we have:

$$\varepsilon_{11} = \frac{1}{\Delta}(T_{11} C_{22} - T_{12} C_{12}), \quad \varepsilon_{22} = \frac{1}{\Delta}(-T_{11} C_{12} + T_{22} C_{11}), \quad \varepsilon_{12} = \frac{1}{C_{66}} T_{12}, \quad \Delta = C_{11} C_{22} - C_{12}^2.$$

Then the component V_i of functional (2) takes the form

$$V = \frac{1}{2}\int_0^L \int_0^{2\pi} \left[\left(\frac{\partial u}{\partial x} + \frac{1}{2}\theta_1^2 \right) T_{11} + \left(\frac{\partial v}{\partial x} + \frac{\partial u}{\partial y} + \theta_1 \theta_2 \right) T_{12} + \left(\frac{\partial v}{\partial y} + \frac{1}{2}\theta_2^2 \right) T_{22} \right.$$

$$- \frac{1}{C_{11} C_{22} - C_{12}} (C_{22} T_{11}^2 + C_{11} T_{22}^2 - 2 C_{12} T_{11} T_{22}) - \frac{1}{C_{66}} T_{12}^2 + C_{13} \left(\theta + \frac{\partial w}{\partial x} \right)^2 + C_{23} \left(\psi + \frac{\partial w}{\partial y} \right)^2$$

$$\left. + D_{11} \left(\frac{\partial \theta}{\partial x} \right)^2 + 2 D_{12} \frac{\partial \theta}{\partial x} \frac{\partial \psi}{\partial y} + D_{22} \left(\frac{\partial \psi}{\partial y} \right)^2 + D_{66} \left(\frac{\partial \theta}{\partial y} + \frac{\partial \psi}{\partial x} \right)^2 \right] dx d\varphi. \tag{9}$$

Since expression (9) is valid for both load-bearing layers, the index "2" is omitted. Let us introduce the force function F as

$$T_{11}=\frac{\partial^2 F}{\partial y^2},\quad T_{12}=-\frac{\partial^2 F}{\partial x\partial y},\quad T_{22}=\frac{\partial^2 F}{\partial x^2}. \tag{10}$$

Since the displacements, strains ε_{33}, and forces T_{33} of the core are expressed using formulas (5)–(7), the functions F_1 and F_2, deflections w_1 and w_2, and functions θ_1,θ_2 and ψ_1,ψ_2 are varied in the functional of the Lagrange principle (1). Then the variational equation becomes

$$\sum_{i-1}^{2}\int_0^L\int_0^{2\pi}\left\{\left[L_1(w_i,F_i)+\frac{1}{R_i}\frac{\partial^2 w_i}{\partial x^2}-\frac{1}{2}(w_i,w_i)\right]\delta F_i+\left[L_2(w_i,F,\theta_i,\psi_i)+(F_i,w_i)+q_i\right]\delta w_i\right.$$

$$\left.+L_3(\theta_i,\psi_i,w_i)\delta\theta_i+L_4(\theta_i,\psi_i,w_i)\delta\psi_i\right\}R_i\,dx\,d\varphi-\sum_{i=1}^{2}\int_0^{2\pi}\left[\left(\frac{1}{R_i^2}\frac{\partial^2 F_i}{\partial\psi^2}+T_{11,0}^i\right)\delta w\right]_0^L R_i\,d\varphi=0. \tag{11}$$

It is assumed that the shell is acted upon by external pressure q_1 applied to the surface of the first layer and by the pressure q_2 caused by the liquid or gas in the second cylinder. In (11), the notation of the differential operators $L_i(\,)$ of the unknown functions is used:

$$L_1(\,)=\left(A_{11}\frac{\partial^4}{\partial x^4}+2A_{12}\frac{\partial^4}{R^2\partial x^2\partial\varphi^2}+A_{22}\frac{\partial^4}{R^4\partial\varphi^4}\right)F_i+\frac{1}{R_i}\frac{\partial^2 w_i}{\partial x^2},$$

$$L_2(\,)=\left[D_{11}\frac{\partial^3}{\partial x^3}+\frac{1}{R^2}(D_{12}+2D_{16})\frac{\partial^3\theta}{\partial x\,\partial\varphi^2}\right]\theta_i+\left[\frac{1}{R_i}(D_{12}+2D_{66})\frac{\partial^3}{\partial x^2\partial\varphi}+\frac{1}{R_i^3}\frac{\partial^3}{\partial\varphi^3}\right]\psi_i$$

$$+\frac{1}{R_i}\frac{\partial^2 F_i}{\partial x^3}-(-1)^i C_3(w_2-w_1)\frac{R_3}{R_i},$$

$$L_3(\,)=\left(D_{11}\frac{\partial^2}{\partial x^2}+\frac{1}{R_i^2}D_{66}\frac{\partial^2}{\partial\varphi^2}\right)\theta_i+\frac{1}{R_i}(D_{12}+D_{66})\frac{\partial^2\psi_i}{\partial x\partial\varphi}-C_{55}\left(\theta_i+\frac{\partial w_i}{\partial x}\right),$$

$$L_4(\,)=\frac{1}{R_i}(D_{12}+D_{66})\frac{\partial^2\theta_i}{\partial x\partial\varphi}+\left(D_{66}\frac{\partial^2}{\partial x^2}+\frac{1}{R_i^2}D_{22}\frac{\partial^2}{\partial\varphi^2}\right)\psi_i-C_{44}\left(\psi_i+\frac{1}{R_i}\frac{\partial w_i}{\partial\varphi}\right). \tag{12}$$

The expression for L_1 includes the following coefficients:

$$A_{11}=\frac{C_{11}}{\Delta},\quad A_{12}=\frac{1}{2}\left(\frac{1}{C_{66}}-\frac{2C_{12}}{\Delta}\right),\quad A_{66}=\frac{C_{22}}{\Delta},\quad \Delta=C_{11}C_{22}-C_{12}^2.$$

The operator "(,)" of the functions F and w can be represented as

$$(F,w)=\frac{1}{R^2}\frac{\partial^2 F}{\partial\varphi^2}\frac{\partial^2 w}{\partial x^2}-\frac{2}{R^2}\frac{\partial^2 F}{\partial x\partial\varphi}\frac{\partial w}{\partial x\partial\varphi}+\frac{1}{R^2}\frac{\partial^2 F}{\partial x^2}\frac{\partial^2 w}{\partial\varphi^2}.$$

Equating the expressions multiplying the variations $\delta F_i,\delta w_i,\delta\theta_i,\delta\psi_i$ in (11) to zero, we get eight nonlinear differential equations

$$L_1(F_i)+\frac{1}{2}(w_i, w_i)=0, \quad L_2(\theta_i, \psi_i)+(F_i, w_i)=q,$$

$$L_3(\theta_i, \psi_i, w_i)=0, \quad L_4(\theta_i, \psi_i, w_i)=0 \quad (i=1,2). \tag{13}$$

These equations can be used to study the stress–strain state of a shell throughout the entire deformation trajectory including limiting points, bifurcation points, and post-buckling behavior.

2. Subcritical State of the Shell. In the above model of a sandwich shell, each load-bearing layer has as many free degrees of freedom as an individual layer without constraints typical for a sandwich. This allowing specifying the load applied to the shell as distributed over the layers. In the problem being considered, the outer layer (i = 1) is acted upon by compressive pressure q_1, while the inner layer (i = 2) undergoes pressure q_2 of opposite sign. It is assumed that the ends are hinged and free of load. If the subcritical state is momentless, then it follows from (1) with (2)–(8) that

$$T_{22,1}=-C_{22}\frac{w_1}{R_1}, \quad T_{22,2}=-C_{22}\frac{w_2}{R_2},$$

$$-C_{22}\frac{w_1}{R_1^2}+C_3(w_2-w_1)\frac{R_3}{R_1}=-q_1,$$

$$-C_{22}\frac{w_2}{R_2^2}-C_3(w_2-w_1)\frac{R_3}{R_2}=-q_2.$$

Solving this system, we find the subcritical forces

$$T_{22,1}=-\lambda a_q^{(1)}, \quad T_{22,2}=-\lambda a_q^{(2)},$$

where

$$\lambda=q_1R_1, \quad a_q^{(1)}=1-\omega, \quad a_q^{(2)}=-\frac{q_2R_2}{q_1R_1}+\omega, \quad \omega=\frac{C_3R_1R_3\left(1+\dfrac{q_2R_2^2}{q_1R_1^2}\right)}{C_{22}+C_3R_3(R_1+R_2)}.$$

Solving the homogeneous problem (17), (18) for the given coefficients $a_q^{(1)}$ and $a_q^{(2)}$, we find either the critical value of the parameter λ_c or the critical intensity of the external pressure q_1^c. The critical values of deflections w_1 and w_2 are defined by

$$w_1=\lambda_cR_1a_q^{(1)}/C_{22},$$

$$w_2=\lambda_cR_2a_q^{(2)}/C_{22}. \tag{14}$$

These deflections can be used to estimate how the distance between the load-bearing layers varies before bifurcation. This determines the value of the constant of interfacial interaction [7].

3. Asymptotic Analysis of Nonlinear Equations. Having determined the stress state of the shell, we calculate the critical load and determine the initial post-critical behavior of the shell in the vicinity of the critical point. To this end, we will use the asymptotic Koiter method [8] in Budiansky's alternative form [5, 6]. Suppose that the load applied to the shell varies proportionally to the parameter λ, while the bifurcation load is determined by the parameter λ_q. After passing the bifurcation point, the equilibrium state of the shell is determined by the changed value of the parameter λ that can be described by

$$\lambda=\lambda_c(1+a\xi+b\xi^2+\dots). \tag{15}$$

Thus, if the values of the parameter λ_c and the coefficients a and b of the series (14) are known, the post-buckling behavior of the shell can be determined using the theory [8]. Following [6], we will expand the unknown functions in (13) into asymptotic series in powers of a small parameter:

$$\begin{bmatrix} F_i \\ w_i \\ \theta_i \\ \psi_i \end{bmatrix} = \begin{bmatrix} F_{i,0} \\ 0 \\ 0 \\ 0 \end{bmatrix} + \xi \begin{bmatrix} F_{i,1} \\ w_{i,1} \\ \theta_{i,1} \\ \psi_{i,1} \end{bmatrix} + \xi^2 \begin{bmatrix} F_{i,2} \\ w_{i,2} \\ \theta_{i,2} \\ \psi_{i,2} \end{bmatrix} + \xi^3 \begin{bmatrix} F_{i,3} \\ w_{i,3} \\ \theta_{i,3} \\ \psi_{i,3} \end{bmatrix}, \tag{16}$$

where ξ is the small amplitude of the buckling mode, the first index i denotes the layer number ($i = 1, 2$), the second one, the term number in the series.

Substituting (16) into (11) and equating the expressions multiplying the parameter ξ to different powers to zero, we obtain a sequence of problem statements for the functions that are the coefficients of series (16). In the case of the first power, we have a variational equilibrium equation at the point where the main trajectory intersects with the trajectory of another solution of the nonlinear equations. The homogeneous problem for the functions with index "1" is derived from the equation

$$\sum_{i=1}^{2} \int_0^L \int_0^{2\pi} \Big\{ L_1\Big(F_{i,1}, \dots\Big)\, \delta F_{i,1} + \Big[L_2\,(F_{i,1}, \dots) + \lambda_c\,(F_{i,0}, w_{i,1}) \Big] \delta w_{i,1}$$

$$+ L_3\,(w_{i,1}, \dots)\, \delta\theta_{i,1} + L_4\,(w_{i,1}, \dots)\, \delta\psi_{i,1} \Big\} R_i\, dx d\varphi = 0, \tag{17}$$

where the bracket "(,)" takes the form

$$\lambda(F_{i,0}, w_{i,1}) = -\lambda_c a_q \frac{\partial^2 w_{i,1}}{R_i^2 \partial \varphi^2}. \tag{18}$$

The variations of the function in (17) can take values of the coefficients in (16). As a result, we obtain the following orthogonality relations:

$$\sum_{i=1}^{2} \int_0^L \int_0^{2\pi} \Big\{ L_1\Big(F_{i,1}, w_{i,1}\Big)\, F_{i,n} + \Big[L_2\,(F_{i,1}, \dots) - \lambda(F_{i,1}, w_{i,1}) \Big] w_{i,n}$$

$$+ L_3\,(w_{i,1}, \dots)\, \theta_{i,n1} + L_4\,(w_{i,1}, \dots)\, \psi_{i,n} \Big\} R_i\, dx d\varphi = 0. \tag{19}$$

This condition yields another form of this relation:

$$\sum_{i=1}^{2} \int_0^L \int_0^{2\pi} \Big\{ L_1\Big(F_{i,n}, w_{i,n}\Big)\, F_{i,1} + \Big[L_2\,(F_{i,n}, \dots) - \lambda(F_{i,n},\, w_{i,1}) \Big] w_{i,1}$$

$$+ L_3\,(w_{i,n}, \dots)\, \theta_{i,1} + L_4\,(w_{i,1}, \dots)\, \psi_{i,1} \Big\} R_i\, dx d\varphi = 0. \tag{20}$$

We use conditions (20) to determine the coefficients a and b in (14). Let us consider a relation from which it is possible to determine the value of a. At ξ^2, we have

$$\sum_{i=1}^{2} \int_0^L \int_0^{2\pi} \Big\{ \Big[L_1\,(F_{i,2}, \dots)\, \frac{1}{2}\Big(w_{i,1},\, w_{i,1}\Big) \Big] F_{i,1} + \Big[L_2\,(w_{i,2}, \dots) - a\lambda_c\,(F_{i,0}, w_{i,2}) + (F_{i,1}, w_{i,2}) \Big] w_{i,1}$$

$$+ L_3\Big(w_{i,2} \dots\Big)\, \theta_{i,1} + L_4\Big(w_{i,2}, \dots\Big)\, \psi_{i,1} \Big\} R_i\, dx d\varphi = 0. \tag{21}$$

Considering condition (20) at $n = 2$ and the equality

$$\int_0^{2\pi}\int_0^{L}\left[\frac{1}{2}(w_{i,1}, w_{i,1})F_{i,1} + (F_{i,1}, w_{i,1})w_{i,1}\right]R_i\,dxd\varphi = 0,$$

we find from (21) that $a = 0$.

The similar integral at ξ^3 takes the form

$$\sum_{i=1}^{2}\int_0^{2\pi}\int_0^{L}\left\{\left[L_1\left(F_{i,3}, \ldots\right) + (w_{i,1}, w_{i,2})\right]F_{i,1} + \left[L_2(w_{i,3}, \ldots) - \lambda_c(F_{i,0},\, w_{i,3}) + (F_{i,1},\, w_{i,2}) + \left(F_{i,2}, w_{i,1}\right)\right.\right.$$

$$\left.\left. - \lambda_c b(F_{i,o},\, w_{i,1})\right]w_{i,1} + L_3(w_{i,3} \ldots)\theta_{i,1} + L_4(w_{i,3}, \ldots)\psi_{i,1}\right\}R_i\,dxd\varphi = 0.$$

With the orthogonality condition, from (20) we get

$$\sum_{i=1}^{2}\int_0^{2\pi}\int_0^{L}\left\{\left(w_{i,1}, w_{i,2}\right)F_{i,1} + \left[(F_{i,1}, w_{i,2}) + \left(F_{i,2},\, w_{i,1}\right)\right]w_{i,1} - \lambda_c b(F_{i,o},\, w_{i,1})w_{i,1}\right\}R_i\,dxd\varphi = 0.$$

With these equations, we can determine the coefficient b describing the initial post-buckling behavior of the shell. Using the solutions of the homogeneous problem (17) and inhomogeneous one (21), we get

$$-b = \frac{B}{\lambda_c A}, \tag{22}$$

where

$$B = \sum_{i=1}^{2}\int_0^{L}\int_0^{2\pi}\left\{\left[\left(w_{i,1},\, w_{i,2}\right)F_{i,1} + (F_{i,1}, w_{i,2})\right]w_{i,1} + (F_{i,2}, w_{i,1})\,w_{i,1}\right\}R_i\,dxd\varphi,$$

$$A = \sum_{i=1}^{2}\int_0^{L}\int_0^{2\pi}(F_{i,0},\, w_{i,1})\,w_{i,1}R_i\,dxd\varphi. \tag{23}$$

4. Solving the Problem of Stability and Initial Post-Buckling Behavior. To calculate the critical load parameter λ_c, we will employ the variational equation (17). Given boundary conditions, the solution can be represented by one term of a trigonometric series due to the constancy of the coefficients of the unknown functions:

$$F_{i,1} = B^{(i)}\sin l_m x\cos n\varphi, \qquad w_{i,1} = C^{(i)}\sin l_m x\cos n\varphi,$$

$$\theta_{i,1} = D^{(i)}\cos l_m x\cos n\varphi, \qquad \psi_{i,1} = E^{(i)}\sin l_m x\sin n\varphi \tag{24}$$

for the first ($i = 1$) and second ($i = 2$) layers,

$$l_m = \frac{m\pi}{L}, \qquad m = 1, 2, \ldots, \qquad n = 2, 3, \ldots.$$

Substituting (24) into (17) and carrying out the necessary procedures, we arrive at a system of homogeneous algebraic equations:

$$[X_{ij}]\overline{Y} = 0, \quad i, j = 1, \ldots, 8, \quad \overline{Y} = (B^{(1)}, C^{(1)}, D^{(1)}, E^{(1)}, B^{(2)}, C^{(2)}, D^{(2)}, E^{(2)}), \tag{25}$$

where

$$X_{11} = A_{11} l_m^4 + 2A_{12} l_m^2 n_1^2 + A_{26} n_1^3, \quad X_{12} = \frac{1}{R_1} l_m^2, \quad X_{21} = X_{12}, \quad X_{22} = -\frac{R_3}{R_1} C_3,$$

$$X_{23} = D_{11} l_m^3 + (D_{12} + 2D_{66}) l_m n_1^2, \quad X_{24} = -(D_{12} + 2D_{66}) l_m^2 n_1, \quad X_{26} = -\frac{R_3}{R_1} C_3,$$

$$X_{32} = -C_{55} l_m, \quad X_{33} = -D_{11} l_m^2 - D_{66} n_1^2, \quad X_{34} = (D_{12} + D_{66}) l_m n_1,$$

$$X_{42} = C_{44} n_1, \quad X_{43} = X_{34}, \quad X_{44} = -D_{66} l_m^2 - D_{22} n_1^2, \quad n_1 = \frac{n}{R_1}.$$

The coefficients X_{ij} at $i = 5, \ldots, 8$ are calculated by the same formulas where R_1 is replaced by R_2, and i, j by $(i + 4)$, $(j + 4)$, except for X_{26} because $X_{62} = -(R_3 / R_2) C_3$. Let us reduce the eight equations of system (25) to two equations:

$$\left[-\frac{X_{12}^2}{X_{11}} + X_{22} + X_{23} \frac{\Delta_1'}{\Delta'} + X_{24} \frac{\Delta_2'}{\Delta'} + \lambda (a_t' l_m^2 + a_q' n_1^2) \right] C^{(1)} + X_{26} C^{(2)} = 0,$$

$$X_{26} C^{(1)} + \left[-\frac{X_{56}^2}{X_{55}} + X_{66} + X_{67} \frac{\Delta_1''}{\Delta''} + X_{68} \frac{\Delta_2''}{\Delta''} + \lambda (a_t l_m^2 + a_q n_2^2) \right] C^{(2)} = 0, \tag{26}$$

where $\Delta' = X_{33} X_{44} - X_{34}^2$, $\Delta_1' = -X_{32} X_{34} + X_{42} X_{43}$, $\Delta_2' = -X_{33} X_{42} + X_{32} X_{43}$. The expressions for $\Delta'', \Delta_1'', \Delta_2''$ remain the same if i, j are replaced by $(i + 4)$, $(j + 4)$.

Equations (26) are used to determine the critical parameter value λ_c and wave numbers m and n that define the bifurcation buckling mode. In writing the system of equations for the functions with index "2", we keep only the 1th, 2th, 5th, and 6th equations because the 3th, 4th, 7th, and 8th equations remain homogeneous and of the same form as in the previous problem. At $a = 0$, we have

$$L_1 (F_{i,2}) = \frac{1}{2} (w_{i,1}, w_{i,1}),$$

$$L_2 (w_{i,2}, \ldots) - \lambda_c (F_{i,0}, w_{i,1}) = -(F_{i,1}, w_{i,1}). \tag{27}$$

At $i = 1$, we arrive at the 1th and 2th equations of the original system, while at $i = 2$ we arrive at the 5th and 6th equations. Substituting (24) for the bifurcation functions $w_{i,1}$ and $F_{i,1}$ into (27), we get the right-hand sides

$$\frac{1}{2} (w_{i,1}, w_{i,1}) = \gamma_1^{(i)} \left(\sum_k b_k \sin l_k x - \cos 2n\varphi \sum_k c_k \sin l_k x \right),$$

$$(F_{i,1}, w_{i,1}) = \gamma_2^{(i)} \left(\sum_k b_k \sin l_k x - \cos 2n\varphi \sum_k c_k \sin l_k x \right), \tag{28}$$

where

$$\gamma_1^{(i)} = \frac{1}{2} (C^{(i)})^2 l_m^2 n^2, \quad \gamma_2^{(i)} = B^{(i)} C^{(i)} l_m^2 n_1^2,$$

$$b_k = \frac{4k}{\pi (k^2 - 4m^2)}, \quad c_k = \frac{4}{n\pi}, \quad k = 1, 3, \ldots.$$

The solution of Eqs. (27) is represented as

$$F_{i,2} = \sum_k B_{k,0}^{(i)} \sin l_k x + \cos 2n\varphi \sum_k B_{k,2n}^{(i)} \sin l_k x,$$

$$w_{i,2} = \sum_k C_{k,0}^{(i)} \sin l_k x + \cos 2n\varphi \sum_k C_{k,2n}^{(i)} \sin l_k x,$$

$$\theta_{i,2} = \sum_k D_{k,0}^{(i)} \cos l_k x + \cos 2n\varphi \sum_k D_{k,2n}^{(i)} \cos l_k x,$$

$$\psi_{i,2} = \sin 2n\varphi \sum_k E_{k,2n}^{(i)} \sin l_k x. \tag{29}$$

This solution includes axisymmetric and nonaxisymmetric components, the latter having double number of waves occurring in bifurcation. The system of algebraic equations for the coefficients of series (29) splits into independent systems for each value of k. The matrix of the subsystems takes the form (26). The system of two inhomogeneous equations can be derived in the same way. The coefficients of the axisymmetric component in (29) are found by solving the system

$$(\lambda_{k,0}^{(1)} - \lambda_c T_{11,0}^{(1)} l_k^2) C_{k,0}^{(1)} - \frac{R_3}{R_1} C_3 C_{k,0}^{(2)} = -(\gamma_2^{(1)} + A_{11} l_k^2 \gamma_1^{(1)}),$$

$$-\frac{R_3}{R_2} C_3 C_{k,0}^{(1)} + (\lambda_{k,0}^{(2)} - \lambda_c T_{11,0}^{(2)} l_k^2) C_{k,0}^{(2)} = -(\gamma_2^{(2)} + A_{11} l_k^2 \gamma_1^{(2)}), \tag{30}$$

where

$$\lambda_{k,0}^{(i)} = \frac{C_{55} D_{11} l_k^4}{C_{55} + D_{11} l_k^3} + \frac{1}{A_{11} R_i^2} + \frac{R_3}{R_i} C_3. \tag{31}$$

The coefficients $B_{k,0}^{(i)}$ are determined by

$$B_{k,0}^{(i)} = \frac{1}{R_i A_{11} l_k^4} C_{k,0}^{(i)} + \frac{\gamma_1^{(i)}}{A_{11} l_k^4}. \tag{32}$$

A similar system for solving the non-axisymmetrical problem is

$$\left[\lambda_{k,2n}^{(1)} - \lambda_c \left(T_{11,0}^{(1)} l_k^2 + T_{22,0}^{(1)} (2n_1^2)^2\right)\right] C_{k,2n}^{(1)} - \frac{R_3}{R_1} C_3 C_{k,2n}^{(2)} = \gamma_2^{(2)} + \frac{X_{12}}{X_{11}} \gamma_1^{(1)},$$

$$-\frac{R_3}{R_1} C_3 C_{k,2n}^{(1)} + \left[\lambda_{k,2n}^{(2)} - \lambda_c \left(T_{11,0}^{(2)} l_m^2 + T_{22,0} (2n_2)^2\right)\right] C_{k,2n}^{(2)} = \gamma_2^{(2)} + \frac{X_{56}}{X_{55}} \gamma_1^{(2)}, \tag{33}$$

where $\lambda_{k,2n}^{(1)} = \frac{X_{12}^2}{X_{11}} - X_{22} - X_{33} \frac{\Delta_1'}{\Delta'} - X_{23} \frac{\Delta_2'}{\Delta'}$, while $\lambda_{k,2n}^{(2)}$ and $X_{i,j}$ are calculated by the same replacement as above.

Solving the homogeneous system of equations (17) and inhomogeneous system (27), we determine, using (23), the coefficient b which allows us to ascertain the initial post-buckling behavior of shells (9).

The numerator in Eq. (22) is represented as

$$B_i = \sum_{i=1}^{2} \int_0^L \int_0^{2\pi} \left[\frac{R}{R_i^2} \left(\frac{\partial^2 F_{i,1}}{\partial \varphi^2} \frac{\partial w_{i,1}}{\partial x} - \frac{\partial^2 F_{i,1}}{\partial x \partial \varphi} \frac{\partial w_{i,1}}{\partial \varphi} \right) \frac{\partial w_{i,2}}{\partial x} \right.$$

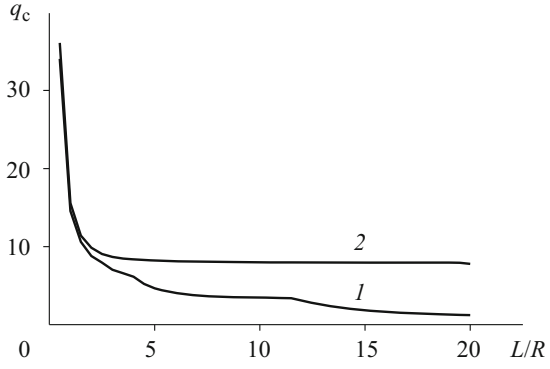

Fig. 1

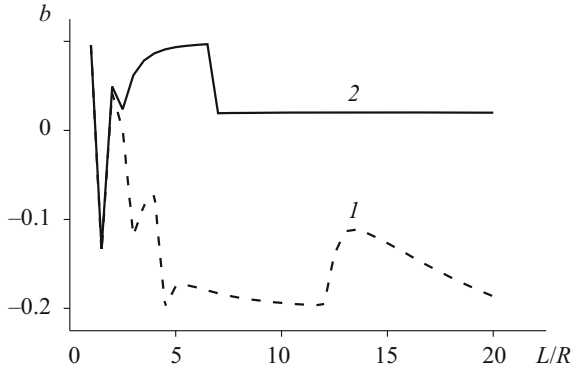

Fig. 2

$$+\frac{2}{R_i^2}\left(\frac{\partial^2 F_{i,1}}{\partial x^2}\frac{\partial w_{i,1}}{\partial \varphi}-\frac{\partial^2 F_{i,1}}{\partial x\partial \varphi}\frac{\partial w_{i,1}}{\partial x}\right)\frac{\partial w_{i,2}}{\partial \varphi}$$

$$+\frac{1}{R_i^2}\left(\frac{\partial w_{i,1}}{\partial x}\right)^2\frac{\partial^2 F_{i,2}}{\partial \varphi^2}+\frac{1}{R_i^2}\left(\frac{\partial w_{i,1}}{\partial \varphi}\right)^2\frac{\partial^2 F_{i,2}}{\partial x^2}-\frac{2}{R_i^2}\left(\frac{\partial w_{i,1}}{\partial \varphi}\frac{\partial w_{i,1}}{\partial x}\right)\frac{\partial^2 F_{i,2}}{\partial x\partial \varphi}\Bigg]R_i\,dx d\varphi\,. \tag{34}$$

When the hoop force λa_q acts, the denominator is given by

$$A_i=-\lambda_c\sum_{i=1}^{2}\int_0^{2\pi}\int_0^{L}a_q^i\left(\frac{\partial w_{i,1}}{R_i\partial \varphi}\right)^2 R_i\,dx d\varphi\,. \tag{35}$$

Then

$$b=-\frac{(B_1+B_2)}{(A_1+A_2)}. \tag{36}$$

The functions $w_{i,1}, w_{i,2}, F_{i,1}, F_{i,2}$ represented by the trigonometric functions (32) and trigonometric series (29) become known after solving the homogeneous system of algebraic equations (26) and inhomogeneous system (33). Substituting these functions into Eqs. (34) and (35) and integrating them, we arrive at the following expressions for the numerator and denominator in (22):

$$B=-2n^2 l_m^2\sum_{i=1}^{2}\left\{\frac{1}{R_i^2}\sum_k\left[2\left(2\frac{B^{(i)}}{C^{(i)}}C_{k,0}+B_{k,0}\right)\frac{k}{4m^2-k^2}+\left(2\frac{B^{(i)}}{C^{(i)}}C_{k,2n}+B_{k,2n}\right)\frac{1}{k}\right]\right\},$$

$$A=\frac{\pi}{2}\sum_{i=1}^{2}\left(C^{(i)}\frac{n}{R_i}\right)^2 a_q^i.$$

If the value of b is known, we can calculate the critical load λ_s applied to a shell with geometrical imperfections in the form of a buckling mode [8]:

$$\left(1-\frac{\lambda_s}{\lambda_c}\right)^{3/2}=\frac{3}{2}\sqrt{-3b}\,\bar{\xi}\frac{\lambda_s}{\lambda_c},$$

where $\bar{\xi}$ is the amplitude of the initial deflection.

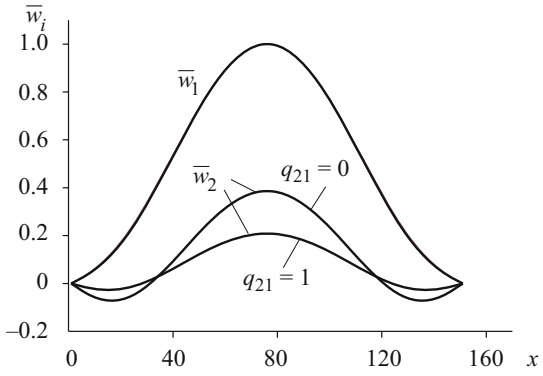

Fig. 3

5. Calculated Results. Let us analyze, as the first example, the stability of double-wall carbon nanotubes (DWCNT) with radius of the outer wall $R_1 = 0.95$ mm and radius of the inner wall $R_2 = 0.61$ mm. These nanotubes are of armchair type ($m = n$). In accordance with the well-known rules, such nanotubes are denoted as [(14, 14), (9, 9)].

The ratio L / R_1 for each case remains the same due to the appropriately chosen length L. The thickness of each wall is equal to 0.066 nm. The mechanical characteristics of the wall are the same as in [13]: $E_1 = 5791.1$ GPa, $E_2 = 7973.5$ GPa, $G_{12} = G_{13} = G_{23} = 1984$ GPa, $\nu = 0.169$.

How the critical intensity of external pressure q_c in double-layer nanotubes depends on the ratio L / R_1 is shown in Fig. 1. If $q_{21} = q_2 / q_1$, then curve *1* corresponds to empty nanotubes ($q_{21} = 0$), while curve *2* corresponds to nanotubes filled with some material that exerts internal pressure q_2, $q_{21} = 1$ [18]. If $_{q21} < 1$, then the corresponding curve is located between those in Fig. 1. Let q_c^e and q_c^f be the critical pressure in empty and filled nanotubes, respectively. In the range $0.5 < L / R_1 < 6$, we have $1 < q_c^e / q_c^f < 2.5$. The buckling modes of empty and filled DWCNTs become different with increasing length (the number of transverse waves is higher for filled nanotubes).

Figure 2 demonstrates how the coefficient of initial post-buckling behavior b varies with the ratio L / R_1. The parameter $C_3 = 89.55$ GPa/nm. Curves *1* and *2* correspond to the same nanotubes as in Fig. 1. The lines are broken and have different slope angles—the coefficient varies stepwise with the length. This behavior of the curves is due to the change of buckling modes. The initial segment of each curve demonstrates frequent change of modes, the frequency decreasing with increasing L / R_1. The greatest difference between curves *1* and *2* is in that the former has negative ordinates at all points, except for the first ones, while the latter has positive ordinates. Since the coordinates in these figures are values of the coefficient b, the critical state of the empty DWCNT is instable, while the critical stated of the filled one is stable. Moreover, as follows from Fig. 1, the critical external pressure for the filled shell is much higher than for the empty shell.

The initial longitudinal post-buckling modes of a DWCNT with $L / R_1 = 2$ are shown in Fig. 3, where all the ordinates of the functions $\overline{w}_i$ are the ratios of the deflections w_i to the maximum deflection w_1 of the upper layer for the empty ($q_{21} = 0$) and filled ($q_{21} = 1$) nanotubes. The deflections of the upper layer w_1 coincide in both cases, while deflections of the inner layer w_2 are different. At $q_{21} = 0$, the deflections $\overline{w}_2$ are concentrated in the shell middle and change the sign near the ends. For $q_{21} = 1$, the amplitudes of the deflections $\overline{w}_2$ decrease and the curve becomes more shallow along the entire length.

Let us consider, as the second example, the stability of sandwich shells whose load-bearing layers are made of carbon-filled plastic with the following mechanical characteristics: $E_1 = 253.4$ GPa, $E_2 = 12.4$ GPa, $G_{12} = G_{13} = 5.04$ GPa, $G_{23} = 4.36$ GPa.

The elastic modulus of the core $E_3 = 1$ MPa, stiffness $C_3 = E_3 / t_3$, the thickness t_3 is equal to $R_1 - R_2 - t$, where R_1 and R_2 are the radii of the upper and inner layers, respectively, t is the thickness of the load-bearing layers.

Let $R_1 = 100$ mm = const and $R_2 = 90$, 80, and 70 mm. The shell length L and thickness t in each case are equal to $2.5R_1$ and 2 mm, respectively. The results obtained are shown graphically in Figs. 4–8. The abscise axis indicates the numbers multiple of which the value of C_3 is.

Figure 4 demonstrates how the critical external pressure q_1 depends on the stiffness C_3 (value of k) for the three cases of the sandwich shell with zero internal pressure ($q_2 = 0$). If the stiffness C_3 is low, the critical loads are maximum for the shell with

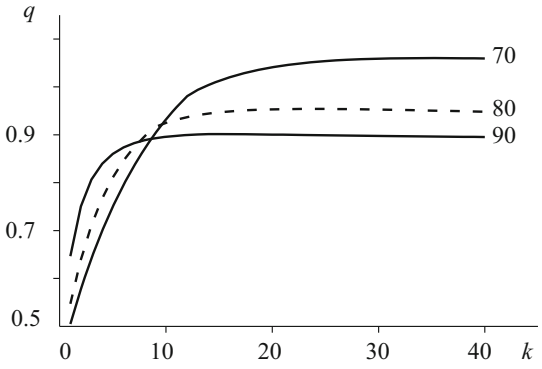

Fig. 4

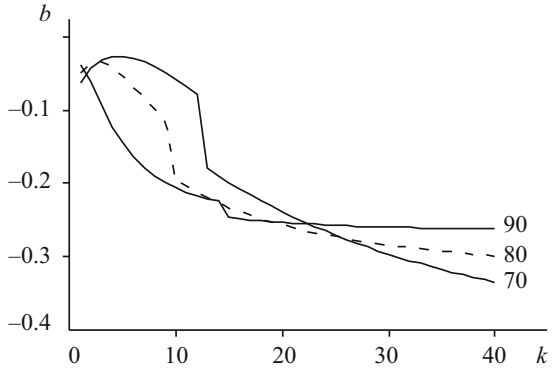

Fig. 5

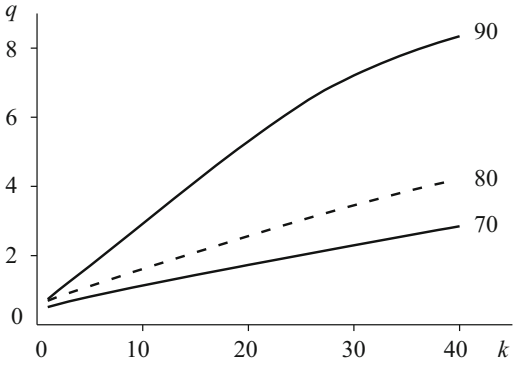

Fig. 6

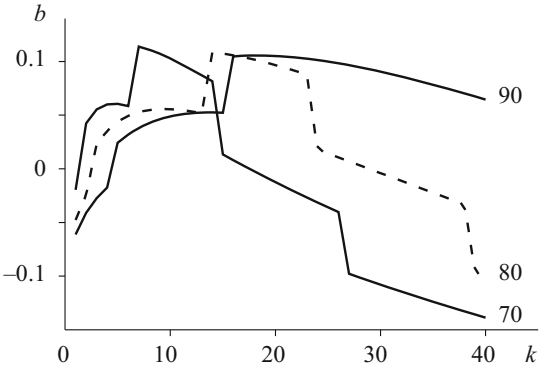

Fig. 7

$R_2 = 90$ mm. However, with increasing stiffness C_3 of the core, the order of arrangement of the curves with $R_2 = 90$, 80, and 70 mm reverses. As is seen from Fig. 4, when $k > 9$, the curve for $R_2 = 70$ mm lies above the other curves, while the curve for $R_2 = 90$ mm lies under the other curves.

The initial post-buckling behavior of the same shells is characterized by Fig. 5, where $b < 0$ for all values of stiffness C_3. Figures 6 and 7 show the calculated values of the critical load and coefficient b for the same sandwich shells acted upon by internal pressure $q_2 = 1$. As can be seen, the critical loads are maximum in the shell with $R_2 = 90$ mm for the above value of the coefficient k of the stiffness C_3. The instability domain of the initial post-buckling behavior of this shell is narrower than for the other two shells. The shell at $k > 4$ with $R_2 = 70$ mm has $b > 0$, which characterizes its insensitivity to imperfections in the form of a buckling mode.

Figure 8 shows how the load-bearing layers of the sandwich shell interact during buckling. The figure illustrates variation in the amplitudes of the buckling modes $C^{(2)}$ (24) of the inner shells with radii $R_2 = 70$, 80, and 90 mm at unit amplitude of the outer shell depending on the parameter k. As is seen, the amplitude $C^{(2)}$ tends to unity with increasing stiffness C_3. When $R_2 = 70$ mm, the load-bearing layers bend so that $C^{(2)} = 1$ in the range of C_3. If $R_2 = 80$ mm or 90 mm at $k > 5$, the curves are very close to the asymptote $C^{(2)} = 1$. The buckling of the sandwich shell as a whole is possible only at a certain value of the transverse stiffness of the core. This value can be determined using the technique described above. It is interesting that if the design model has two reference surfaces, then the buckling modes with different amplitudes of layers can be determined.

Conclusions. We have developed a design model of buckling of sandwich shells with a transversely elastic light core. Its distinctive feature is that the outer and inner cylindrical shells in the sandwich shell demonstrate as many degrees of freedom as those unconnected by the core. This allows describing the loading of individual layers. We have solved the problem of the stability of a sandwich shell acted upon by external pressure applied to the upper layer and oppositely directed to the pressure in the inner cylinder. If the transverse reduction is neglected, the problem becomes trivial. The proposed sandwich shell model can also be considered as a continuous approximation of a double-wall nanotube where the interfacial Van der Waals forces are modeled by a continuum [7]. In contrast to the well-known approaches, our technique is based on the Lagrange variational

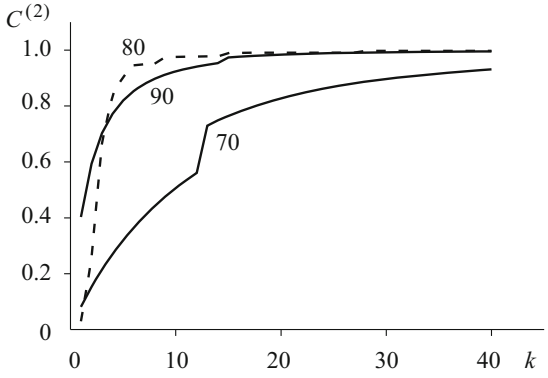

Fig. 8

principle. Consistent nonlinear differential equilibrium equations have been derived. These equations underlie an algorithm for analyzing the stability and post-buckling behavior of a sandwich shell using the asymptotic Koiter–Bydiansky method.

Analyzing the results obtained, we can draw the following conclusions.

The critical intensity of external pressure in the filled double-wall nanotube is higher than that in the empty one. This difference increases with the length of the nanotube. The substantial increase in the critical pressure due to the presence of the filler was established in [18].

An important parameter in analyzing the stability of a double-wall nanotube is the coefficient of post-buckling behavior b, which is negative for the empty nanotube and positive for the filled one. Hence, the critical state is unstable in the former case and is stable in the latter case.

The buckling modes of the outer layer of the empty and filled double-wall nanotubes are close, while those of the core differ substantially because of the pressure that flattens the surface.

We have studied the stability of sandwich shells with carbon-filled plastic load-bearing layers with constant radius of the outer layer and different radii of the inner layer under external pressure. It has been established that when the internal pressure is absent, the critical load increases with transverse stiffness of the core to a certain constant level. The critical load peaks at the minimum radius of the inner layer (70 mm).

If the internal pressure is absent, the coefficient of initial post-buckling behavior of shells with such radii is negative at all values of the stiffness of the core despite the fact that its behavior is different in each case.

If the cylinder with minimum radius in the sandwich is subject to internal pressure, the critical load applied to the shell increases considerably. The internal pressure provides the best support for the shell with radius equal to 90 mm. Shells subject to internal pressure demonstrate stable post-buckling behavior over a wide range of dimensions.

It has been shown that a sandwich shell with a low transverse stiffness losses stability in a mode with equal number of longitudinal and transverse waves for both layers but with different amplitudes. The shapes of the layers in the initial post-buckling state are different.

REFERENCES

1. V. V. Bolotin and Yu. N. Novichkov, *Mechanics of Multilayer Structures* [in Russian], Mashinostroenie, Moscow (1981).
2. G. A. Vanin, N. P. Semenyuk, and R. F. Emel'yanov, *Stability of Reinforced Shells* [in Russian], Naukova Dumka, Kyiv (1978).
3. G. A. Vanin and N. P. Semenyuk, *Stability of Shells Made of Composite Materials with Imperfections* [in Russian], Naukova Dumka, Kyiv (1987).
4. E. I. Grigolyuk, "Equations of sandwich shells with a light core," *Izv. AN SSSR*, *Ser. Techn. Nauki*, No. 1, 77–84 (1957).
5. N. Yamaki, "Postbuckling and imperfection sensitivity of circular cylindrical shells under compression," in: W. T. Koiter (ed.), *Theoretical and Applied Mechanics*, North-Holland, Delft (1976), 461–476.

6. B. Bydiansky, “Theory of buckling and post-buckling behavior of elastic structures,” *Adv. Appl. Mech.*, **14**, 2–65 (1974).
7. X. Q. He, S. Kitipornchai, and K. M. Liew, “Buckling analysis of multi-walled carbon nanotubes: A continuum model accounting for Van Der Waals interaction,” *J. Mech. Phys. Solids*, **53**, 303–326 (2005).
8. W. T. Koiter, “Elastic stability and post-buckling behavior,” in: *Proc. Symp. Nonlinear Problems*, Univ. of Wisconsin Press, Madison (1963), pp. 257–275.
9. V. F. Meish, Yu. A. Meish, and V. F. Pavlyuk, “Dynamics of three-layer elliptical cylindrical shells reinforced with discrete rings,” *Int. Appl. Mech.*, **54**, No. 2, 172–179 (2018).
10. N. P. Semenyuk, “Initial supercritical behavior of fiberglass cylindrical shells with filler under axial compression,” *Int. Appl. Mech.*, **24**, No. 5, 478–484 (1988).
11. N. P. Semenyuk, V. M. Trach, and A. V. Podvornyi, “Spatial stability of layered anisotropic cylindrical shells under compressive loads,” *Int. Appl. Mech.*, **55**, No. 2, 211–221 (2019).
12. N. P. Semenyuk, V. M. Trach, and N. B. Zhukova, “Stability and initial post-buckling behavior of orthotropic cylindrical sandwich shells with unidirectional elastic filler,” *Int. Appl. Mech.*, **55**, No. 6, 636–647 (2019).
13. H. S. Shen, “Postbuckling prediction of double-walled carbon nanotubes under hydrostatic pressure,” *Int. J. Solid Struct.*, **41**, No. 9–10, 2643–2657 (2004).
14. J. X. Shi, T. Natsuki, and Q. Q. Ni, “Radial buckling of multi-walled carbon nanotubes under hydrostatic pressure,” *Appl. Phys.*, *Ser. A*, **117**, No. 3, 1103–1108 (2014).
15. J. R. Vinson, “Sandwich structures: past, present, future, Sandwich structures 7: Advancing in sandwich structures and materials,” in: *Proc. 7th Int. Conf. on Sandwich Structures*, Aalborg Univ., Denmark (2005), pp. 29–31.
16. C. M. Wang, Y. Q. Ma, Y. Zhang, and K. Ang., “Buckling of a double-walled carbon nanotubes modeled by solid shell elements,” *J. Appl. Physics*, **99** (11), 114–117 (2006).
17. C. M. Wang, Y. Y. Zhang, Y. Xiang, and J. N. Reddy, “Recent studies on buckling of carbon nanotubes,” *Appl. Mech. Reviews*, **63**, 1–18 (2010).
18. C. Y. Wang, A. Mioduchowski, and C. Q. Ru, “Critical external pressure for empty or filled multiwall carbon nanotubes,” *J. Comput. Theor. Nanoscie.*, **1**, 1–5 (2005).
19. C. Yuan, O. Bergsma, S. Koussios, et al., “Optimization of sandwich composites fuselages under flight loads,” *Appl. Compos. Mater.*, **19**, No. 1, 47–64 (2012).